

# Pollutant removal, dispersion, and entrainment over two-dimensional idealized street canyons

Colman C.C. Wong and Chun-Ho Liu

Department of Mechanical Engineering, The University of Hong Kong  
Pokfulam Road, Hong Kong, China.

## Abstract

Idealized two-dimensional (2D) street canyon models of unity building-height-to-street-width (aspect) ratio are employed to examine the pollutant transport over hypothetical urban areas. The results show that the pollutant removal is mainly governed by atmospheric turbulence when pollutant sources exist in the street canyons. Numerous decelerating, uprising air masses are located at the roof level, implying that the pollutant is removed from the street canyons to the urban boundary layer (UBL) by ejections. For the street canyons without pollutant source, the removal by ejections is limited leading to insignificant turbulent pollutant removal. The roof-level turbulent kinetic energy (TKE) distribution demonstrates that its production is not governed by local wind shear but the descending TKE from the UBL. In the UBL, the pollutant disperses rapidly over the buildings, exhibiting a Gaussian-plume shape. The vertical pollutant profiles illustrate a self-similarity behavior in the downstream region. Future studies will be focused on the characteristic plume shape over 2D idealized street canyons of different aspect ratios.

## 1. INTRODUCTION

Scalar transport, such as heat, moisture, or pollutants, in the atmospheric boundary layer (ABL) is an attractive research topic with a range of applications. Turbulent transport over a variety of natural terrain has been well explored. For example, Gaussian plume model is able to estimate well the transport of passive scalars over flat and homogeneous terrain (Pasquill, 1983). On the other hand, the mechanism and plume dispersion over urban areas remain as open questions. This study is therefore conceived to examine how urban morphology modifies the pollutant removal, dispersion, and entrainment over urban areas.

## 2. METHODOLOGY

The large-eddy simulation (LES) of the open-source computational fluid dynamics (CFD) code OpenFOAM 1.7.0 (OpenFOAM, 2011) is adopted to calculate the flows over two-dimensional (2D) idealized street canyons in isothermal and incompressible conditions. The modeling details are as follows.

### 2.1 *Computational domain and boundary conditions*

The computational domain consists of 12 identical, idealized 2D street canyons of unity aspect ratio ( $h/b$ , where  $h$  and  $b$  are the building height and street width, respectively) which are

placed evenly in the streamwise direction (Figure 1). Its bottom outlines the ground and the building facades, while the space above the building roofs represents the urban boundary layer (UBL). The dimensions of the spatial domain in the streamwise, spanwise, and vertical directions are  $24h$ ,  $5h$ , and  $8h$ , respectively.

Figure 1 illustrates the computational domain and the boundary conditions of the current LES. A symmetry (free-slip) boundary condition (BC) is applied at the domain top for both flow and pollutant transport. For the flow field, no-slip BCs are applied on the ground and the building facades. A cyclic BC is applied in the horizontal directions in order to simulate the flows over an infinitely wide urban roughness surface. For the pollutant transport, a cyclic BC is applied across the spanwise domain only. In the streamwise direction, zero concentration and an open boundary are applied at the inlet and outlet, respectively. On the ground and the building facades, zero-gradient BCs are used for the pollutant except the ground of the first street canyon where constant pollutant concentration ( $= \Phi$ ) is prescribed. The prevailing wind, which is normal to the street axis, is driven by a background pressure gradient in the UBL only. No pressure gradient is prescribed inside the street canyons.

## 2.2 Numerical method

In the current LES, the implicit second-order accurate backward differencing is employed in the temporal domain. The second-order accurate Gaussian finite volume integration is adopted in the calculation of the gradient, divergence, and laplacian terms. The values on cell faces are interpolated by the central differencing of the values at cell centers. In the spatial discretization,  $32 \times 160 \times 32$  (streamwise  $\times$  spanwise  $\times$  vertical) elements are used in each canyon and  $768 \times 160 \times 280$  elements are used in the UBL, such that the total number of elements exceeds 36 million. The wall-normal distance (in wall unit) of the first grid centroid is around  $z^+ = 5$  that is fine enough resolving the near-wall flows and turbulence using a wall model. The Reynolds number based on the free-stream speed and the building height  $Re (= Uh/\nu)$  is 12,000 and the roughness Reynolds number based on the friction speed  $Re_\tau (= u_\tau h/\nu)$  is 837.

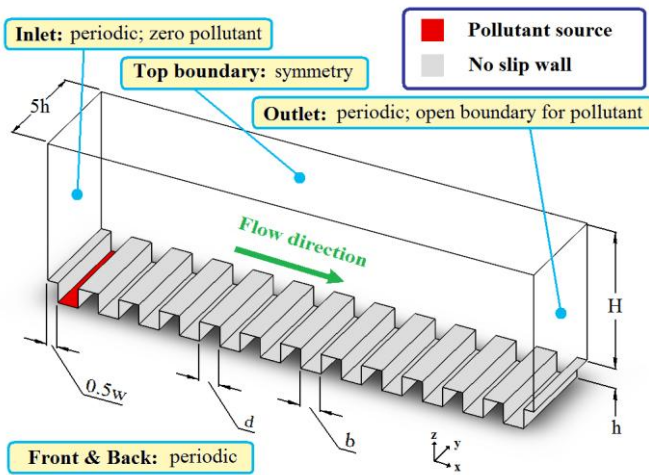


Figure 1. Computational domain and boundary conditions

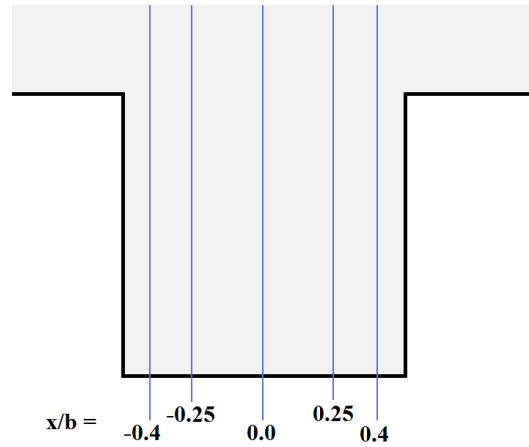


Figure 2. Five segments,  $x/b = -0.4, -0.25, 0, 0.25, \text{ and } 0.4$ , in a street canyon.

### 3. RESULTS

#### 3.1 Flow structure

The flow structure along five vertical segments below and above the roof level of the street canyons (Figure 2) calculated by the current LES are compared with the LES results by Cheng and Liu (2011) and Cui et al. (2004), and the wind tunnel measurements by Brown et al. (2000). The methodology adopted by Cheng and Liu (2011) is very similar to that of the current LES, except a smaller domain, which consists of only 3 identical street canyons, was used that may affect the turbulence structure in the UBL. The LES model of Cui et al. (2004) consists of only one single street canyon in which a different wall model (tangential velocity follows the logarithmic law) is used. The flow and pollutant variables are ensemble averaged in the temporal domain and the spanwise direction. In view of the periodic flow properties in each street canyon, ensemble averaging for the flow variables is also applied on the street canyons (represented by angular parentheses  $\langle \bar{\psi} \rangle$ ). The characteristic velocity  $\langle U_s \rangle$  represents the mean wind speed in the UBL within  $h < z < 1.5h$ . Similarly,  $\text{TKE}_s$  is the characteristic turbulent kinetic energy (TKE), representing the mean TKE in the UBL within  $h < z < 1.5h$ .

Figure 3 compares the vertical profiles of mean flow velocities along the five segments. An isolated, primary recirculation is found spinning inside the street canyon of unity aspect ratio so that the pollutant is transported by the mean flow from the ground level to the leeward side within the street canyon. In the vicinity to the roof level, the mean vertical flow velocity is almost zero, implying that the turbulence governs the pollutant transport in-between the street canyon and the UBL. The vertical profiles of mean streamwise velocity  $\langle \bar{u} \rangle$  agree with those of other studies (Figure 3a). The mean vertical velocity  $\langle \bar{w} \rangle$  also shows a good agreement in the center core of the street canyon ( $x/b = -0.25, 0$ , and  $0.25$ ). Whereas, mild deviations are observed in the near-wall region compared with the LES of Cui et al. (2004) and the wind tunnel measurements of Brown et al. (2000). These dissimilarities could be caused by the coarse spatial resolution in the near-wall region and the different wall models adopted in the studies.

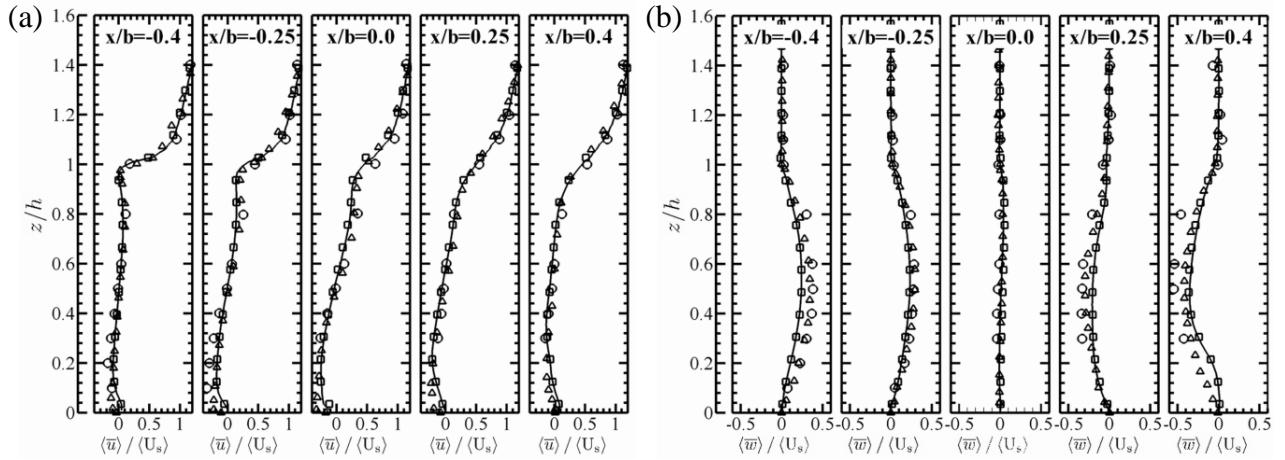


Figure 3. Vertical profiles of the ensemble average of: (a) streamwise velocity  $\langle \bar{u} \rangle / \langle U_s \rangle$ ; (b) vertical velocity

$\langle \bar{w} \rangle / \langle U_s \rangle$ .  $\circ$ : Brown et al. (2000);  $\Delta$ : Cui et al. (2004);  $\square$ : Cheng and Liu (2011); and  $—$ : current LES.

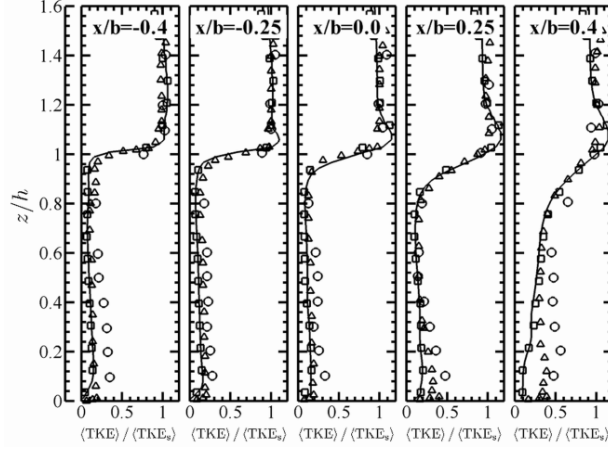


Figure 4. Vertical profiles of the ensemble average of turbulence kinetic energy  $\langle \text{TKE} \rangle / \langle \text{TKE}_s \rangle$ .  $\circ$ : Brown *et al.* (2000);  $\Delta$ : Cui *et al.* (2004);  $\square$ : Cheng and Liu (2011); and —: current LES.

The vertical profiles of the resolved-scale TKE,  $\langle \text{TKE} \rangle = \langle u''u'' + v''v'' + w''w'' \rangle / 2$ , of the current LES is depicted in Figure 4. Here,  $\psi'' = (\bar{\psi} - \langle \bar{\psi} \rangle)$  is the deviation from the ensemble average. The resolved-scale TKE is peaked right above the roof level near the windward facade while the velocity gradient near the leeward facade (Figure 3). The non-overlapping maxima of wind shear and TKE signify the substantial contribution of the descending atmospheric turbulence from the UBL into the street canyons. The current LES-calculated TKE profiles agree reasonably well with other experimental and numerical results except in the vicinity to the windward facade ( $x = 0.4b$ ). It is noteworthy that the turbulence in the LES is solely generated by mechanical shear near the buildings in which the turbulence generated in the upper UBL is likely overlooked. Hence, comparing the turbulence levels in details reveals that LES often under predicts the TKE levels in the near-wall region than those of wind tunnel experiments.

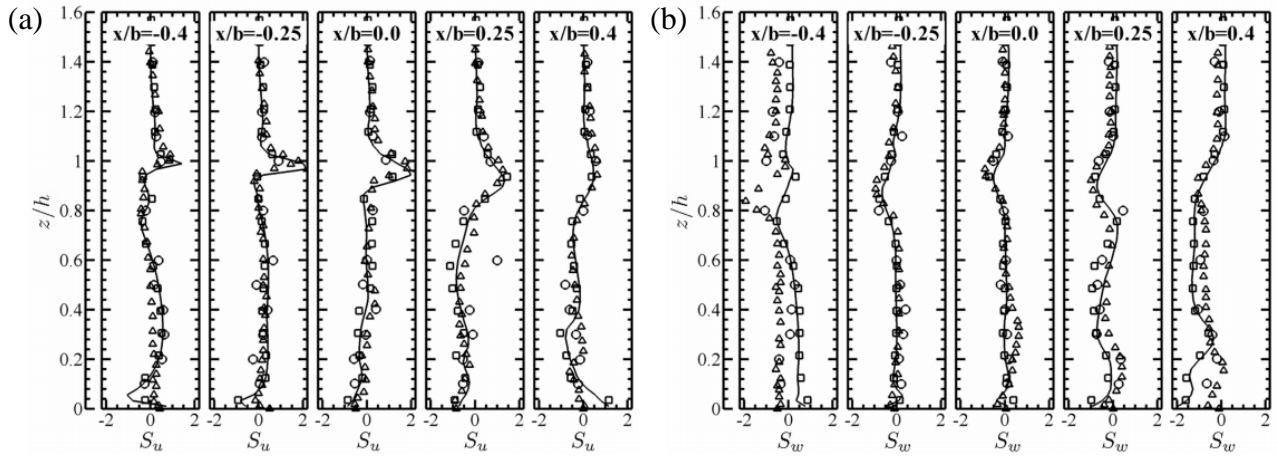


Figure 5. Vertical profiles of the skewness of: (a) the streamwise velocity  $S_u$ ; (b) vertical velocity  $S_w$ .  $\circ$ : Brown *et al.* (2000);  $\Delta$ : Cui *et al.* (2004);  $\square$ : the LES of Cheng and Liu (2011); and —: current LES.

Figures 5 and 6 show the skewness  $S$  and kurtosis  $K$ , respectively, of the velocities. In line with other numerical and experimental results, a layer of positive  $S_u$  is found along the roof level, demonstrating that most of the air masses are decelerating while a few narrow air masses are accelerating. The skewness of the streamwise velocity fits reasonably well with that of other studies. However, the skewness of the vertical velocity shows differences near the building facades that is likely caused by the different mean flow velocities. On the other hand, the kurtosis fits well with others even though it is a 4th-order parameter which is sensitive to the modeling accuracy. Conclusively, the current LES has comparable results with other LESs as well as wind tunnel experiments, suggesting its reliability for street canyon applications.

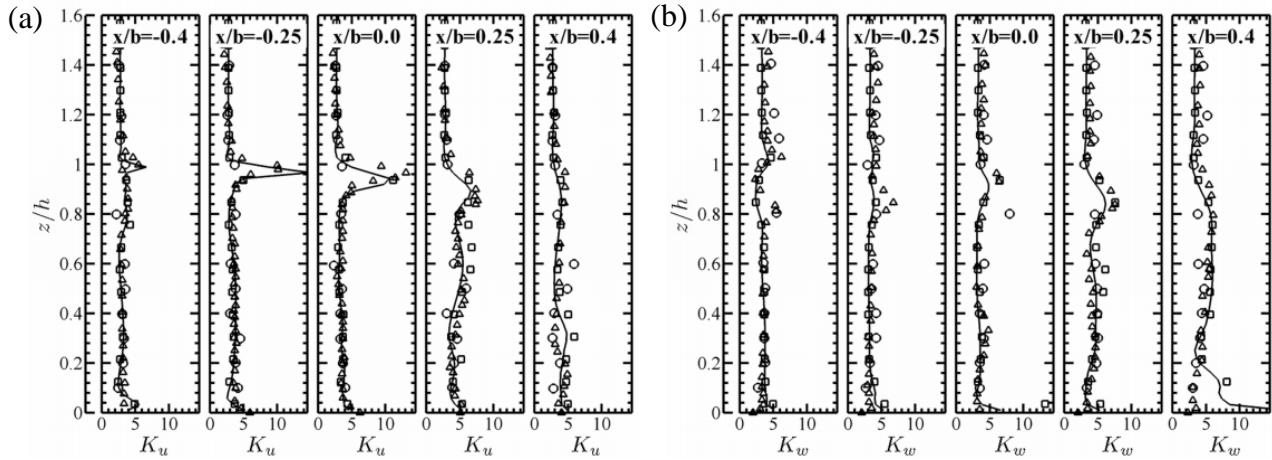


Figure 6. Vertical profiles of the Kurtosis of: (a) the streamwise velocity  $K_u$ ; (b) the vertical velocity  $K_w$ .  $\circ$ : Brown *et al.* (2000);  $\Delta$ : Cui *et al.* (2004);  $\square$ : the LES of Cheng and Liu (2011); and  $—$ : current LES.

### 3.2 Pollutant removal and entrainment

Figure 7a shows the ensemble averaged vertical pollutant flux along the roof level of the first street canyon where a ground-level pollutant source exists. It is clearly depicted that the pollutant is mainly removed out of the street canyon by the turbulent flux. On the other hand, the mean wind carries the pollutant out of the canyons on the leeward side and near the windward building edge, which, however, subsequently drives the pollutant from the UBL back into the street canyon on the windward side. As a result, the net mean pollutant flux diminishes. The mean pollutant flux of the current LES is comparable to that of RANS (Cheng *et al.* 2008). Whereas, the turbulent components are different from each other that is reflected by the dissimilar TKE distributions. Nevertheless, both the current LES and the RANS of Cheng *et al.* (2008) support the transport mechanism that the pollutant removal from a 2D street canyon with ground-level pollutant source is dominated by turbulence transport.

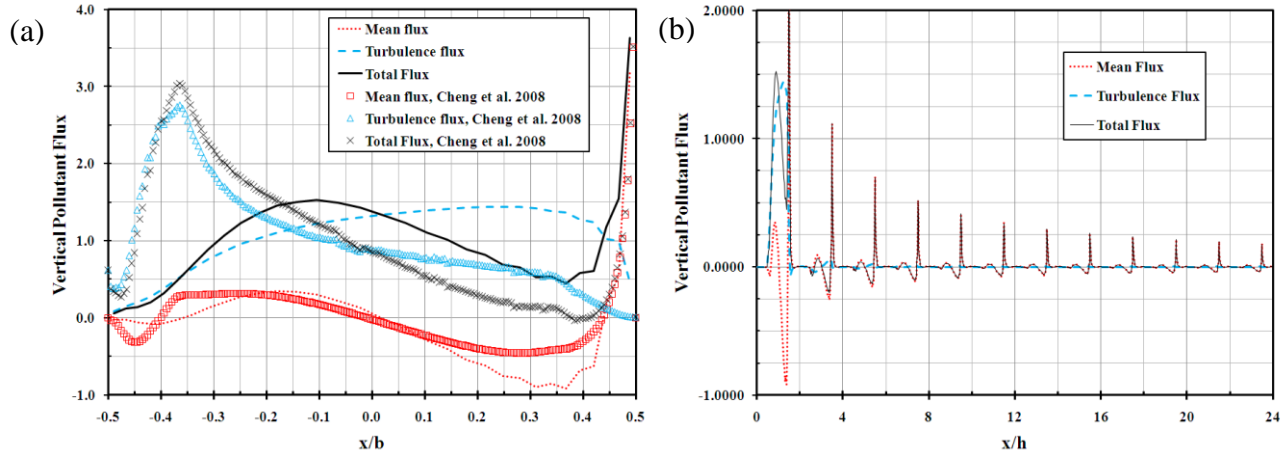


Figure 7. Ensemble average vertical pollutant flux along the roof level: (a) for the first street canyon; (b) for the whole domain. Mean flux  $\langle \bar{\phi} \rangle \langle \bar{w} \rangle / Q_r$ , turbulence flux  $\langle \phi'' w'' \rangle / Q_r$  and total flux  $\langle \phi w \rangle / Q_r$ .  $Q_r$  is the averaged flux at the roof level of first street canyon.

Figure 7b shows the ensemble averaged vertical pollutant flux along the roof level of all the street canyons of the whole spatial domain. For the street canyons without pollutant source, the mean pollutant flux drops with decreasing pollutant concentration, which decreases exponentially in the streamwise direction. On the contrary, the turbulent flux drops quickly down to zero whose transport is insignificant after the third street canyon. Since the turbulent flux contributes to the pollutant removal of the first canyon, while the pollutant concentrations in other street canyons are driven by the mean flux, we hypothesize that the pollutant removal and entrainment are governed, respectively, by turbulence and mean wind.

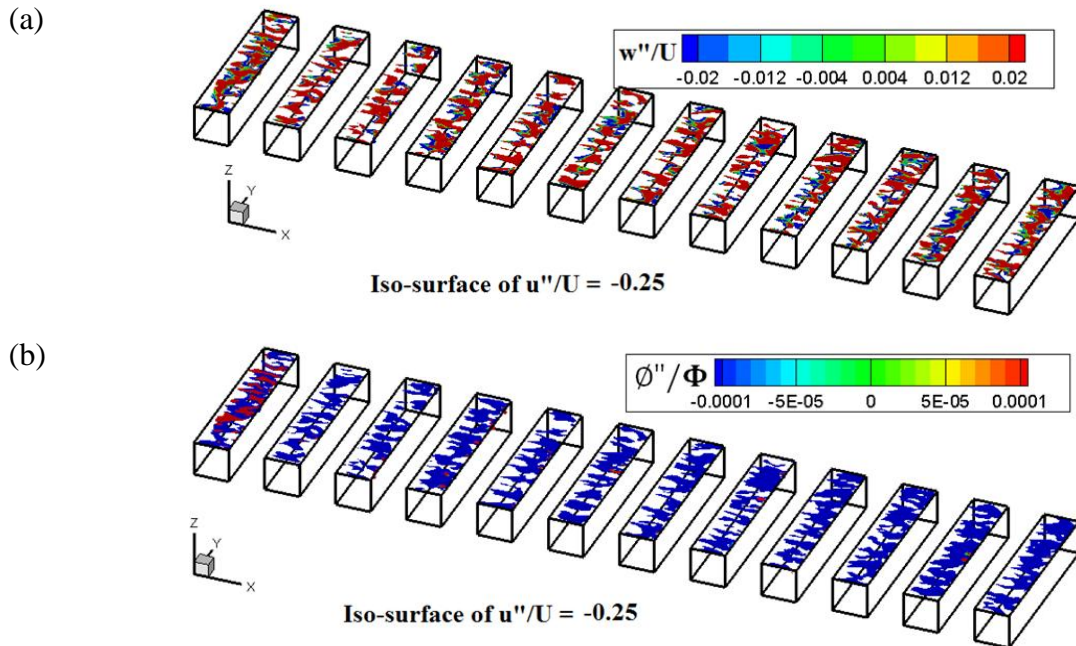


Figure 8. Iso-surface of streamwise fluctuating velocity  $u'' = -0.25U$ . (a): The contours represent the vertical fluctuating velocity  $w''/U$ ; (b): The color contours represent the fluctuating pollutant concentration  $\phi''/\Phi$ .

### 3.3 Removal mechanism on roof level

Coherent structures of the flows and pollutant transport are revealed by the LES that helps elucidate the pollutant removal mechanism over 2D street canyons. As mentioned in the previous section, a layer of positive skewness (Figure 5a) is observed along the roof level, realizing the dominance of decelerating air masses. Figure 8 shows the snap shots of those decelerating air masses  $u'' = -0.25U$ . Most decelerating air masses are moving upward (i.e.  $w'' > 0$ ; Figure 8a) that suggests the turbulent pollutant removal is mainly in the form of ejections. Figure 8b shows that the decelerating, upward moving air masses only carry a smaller amount of pollutant out of the street canyons without pollutant source ( $\phi'' < 0$ ). Therefore, the pollutant removal driven by ejections is rather limited and a similar amount of pollutant is carried back into the street canyon by sweeps. The pollutant de-entrainment and re-entrainment cancel out each other finally, resulting in negligible turbulent pollutant transport. The pollutant transport is thus dominated by the mean flow.

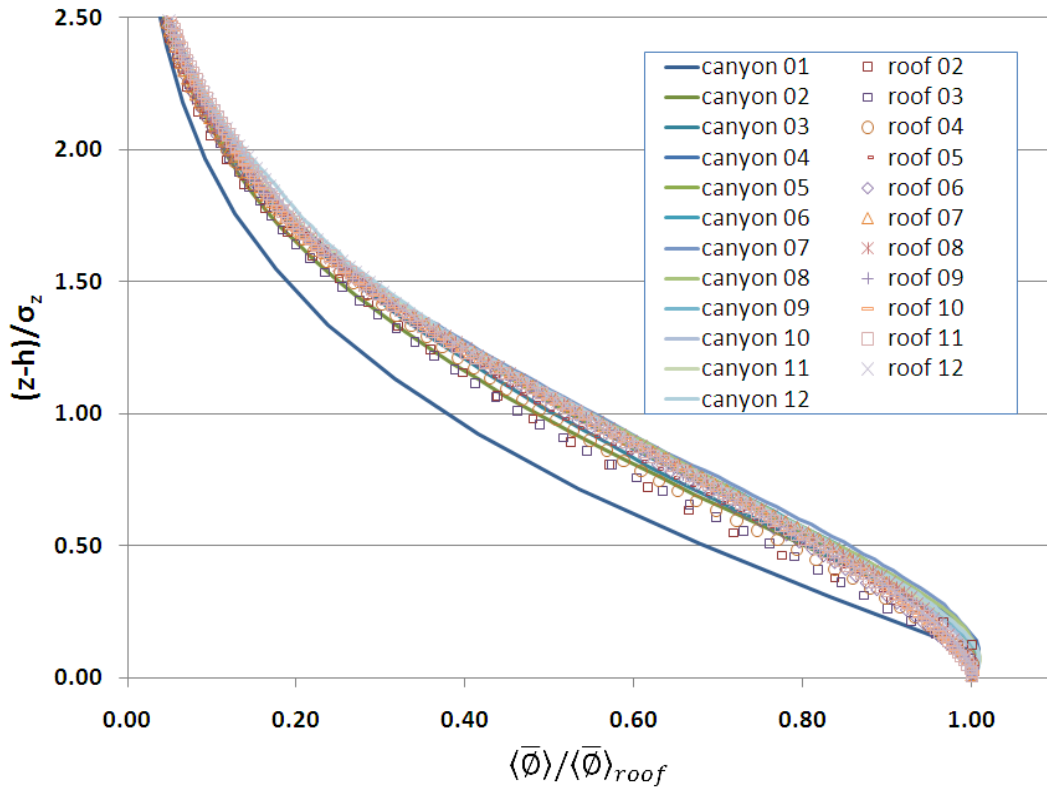


Figure 9. Normalized vertical plume profiles.

### 3.4 Pollutant plume

Davidson *et al.* (1996) proved that the pollutant plume over an array of obstacles exhibits a Gaussian form so, analogously, a Gaussian pollutant plume is expected over idealized 2D street canyons. Figure 9 shows the pollutant concentration profiles along different vertical planes. The normalization method is the same as the Gaussian plume pollutant model, where  $\langle \bar{\phi} \rangle_{roof}$  is the mean pollutant concentration at roof level,

$$\sigma_z^2 = \frac{\iint (z-h)^2 \bar{\phi} dydz}{\iint \bar{\phi} dydz} \quad (1)$$

The vertical plume shape calculated by the current LES closely resembles the Gaussian plume shape. The results also show that after a certain distance away from the pollutant source, the normalized vertical plume profiles achieve self-similarity similar to the Gaussian pollutant plume model. Besides, the plume profiles over the building roofs and the street canyons do not differ too much, implying that the street canyons without pollutant source do not modify too much the plume dispersion aloft.

#### 4. CONCLUSION

An LES pollutant dispersion model over 2D street canyons is developed. It is shown that the pollutant in the street canyons is transported and/or diluted by the primary recirculation. At the roof level, the pollutant removal (entrainment) is mainly governed by turbulence (mean wind) when the pollutant source is present in the street canyon. At the roof level, the decelerating air masses move upward carrying the pollutant out of the street canyons to the UBL by ejections. For street canyon without pollutant source, the pollutant removed by this mechanism is rather limited, which however, is governed by mean flow instead. The pollutant plume in the UBL exhibits self-similarity in the downstream region. Future studies will be focused on the relationship between plume shapes over 2D idealized street canyons of different aspect ratios.

#### 5. ACKNOWLEDGEMENTS

This study was jointly supported by the Strategic Research Areas and Themes, *Computational Sciences*, and the University Research Committee *Seed Funding Programme of Basic Research* 200910159028 of the University of Hong Kong. The computation is supported in part by a Hong Kong UGC Special Equipment Grant (SEG HKU09). The technical support from Lillian Y.L. Chan, Frankie F.T. Cheung, and W.K. Kwan with HKUCC is appreciated.

#### 6. REFERENCES

- Brown MJ, Lawson RE, Decroix DS, Lee RL. 2000. Mean flow and turbulence measurements around a 2-D array of buildings in a wind tunnel. In: Proceedings of the 11th joint AMS/AWMA Conference in Applied Air Pollution Meteorology. Long Beach, CA, USA.
- Cheng, W.C., Liu, C.H., Leung, D.Y.C., 2008. Computational formulation for the evaluation of street canyon ventilation and pollutant removal performance. *Atmospheric Environment* 42, 9041–9051.
- Cheng WC, Liu CH. 2011. Large-eddy simulation of flow and pollutant transport in and above two-dimensional idealized street canyons. *Boundary-Layer Meteorol*, in press.
- Cui ZQ, Cai XM, Baker CJ. 2004. Large-eddy simulation of turbulent flow in a street canyon. *Quarterly Journal of the Royal Meteorological Society* **130**: 1373–1394.
- Davidson MJ, Snyder WH, Lawson RE, Hunt JCR. 1996. Wind tunnel simulations of plume dispersion through groups of obstacle, *Atmospheric Environment*. **30**: 3715-3731.
- OpenFOAM. 2011. OpenFOAM: The open source CFD toolbox. <http://www.openfoam.com/>.
- Pasquill F. 1983. *Atmospheric diffusion*. John Wiley & Sons: New York, USA.